Light-driven molecular machine at ITIES

Light-driven molecular machine at ITIES

Alexei A Kornyshev[1]**, Marina Kuimova**[1]**, Alexander M Kuznetsov**[1,2]**,
Jens Ulstrup**[3] **and Michael Urbakh**[4]

[1] Section of Theoretical and Experimental Physical Chemistry, Department of Chemistry,
Faculty of Natural Sciences, Imperial College of Science, Technology and Medicine,
London SW7 2AZ, UK
[2] Laboratory of Physical Electrochemistry, The A N Frumkin Institute of Physical Chemistry and
Electrochemistry of the Russian Academy of Sciences, 117071 Moscow, Russia
[3] Bioinorganic Chemistry Group, Department of Chemistry and Nano DTU, The Technical
University of Denmark, DK-2700 Kongens Lyngby, Denmark
[4] School of Chemistry, Sackler Faculty of Exact Sciences, Tel Aviv University, Ramat Aviv, 69978
Tel Aviv, Israel

Abstract
We suggest a principle of operation of a new molecular device that transforms
the energy of light into repetitive mechanical motions. Such a device can
also serve as a model system for the study of the effect of electric field on
intramolecular electron transfer. We discuss the design of suitable molecular
systems and the methods that may monitor the 'performance' of such a machine.

1. Introduction

Molecular-scale systems that can be studied and controlled with single-molecule resolution
offer exciting perspectives in routes towards nanotechnology. The creation of molecular-
scale systems in which external stimuli such as chemical reagents, light, or external electric
fields trigger strong conformational transitions is at the forefront of such investigations.
These systems can ultimately be converted to electronic on-off switching, rectification and
amplification devices or integrated into larger assemblies for molecular-scale mechanical
energy conversion.

An immediate example of Nature's own electronically triggered conformational transitions
is the folding and unfolding of redox metalloproteins induced by fast reduction and oxidation,
respectively [1]. ATPase, myosin, and several other enzyme systems are more sophisticated
examples where chemical energy is converted to mechanical work at the true nanometre
scale [2]. The latter systems are, however, based on large biological structures presently far
too complicated for emulation or exploitation in man-made synthetic devices. However, over
the last decade an impressive variety of synthetic supramolecular systems have been brought
into play with an ensemble of functions which could be stimulated by excitation with visible
light [3]. These systems mostly contain transition metal complexes as redox centres with

accessible electronic levels that can be successively populated and depopulated in order to impose a variety of electronic functions. These cover not only single-component 'switching' and other electronic function but also form the basis for more complex supramolecular 'logic gates' or even molecular scale 'circuits'.

Changes in the electronic structure of the transition metal centre caused by an excitation or redox process is but one of the approaches to inducing the drastic changes in the molecular conformation. Chemical reactions can also be used to release a 'punch' or a 'burst' of mechanical energy by altering a subtle balance between non-covalent intermolecular forces among the ligands and/or transition metal centre, e.g. hydrogen bonding or coordination bonding. Translational or rotational mechanical motion of rotaxanes and catenanes following the application of external stimuli is widely used in such architectures [3–6]. Together with a variety of other molecular architectures, these have led to nanoscale replicas of mechanical 'rotors', 'gears', 'paddle wheels', 'tweezers', 'harpoons' etc [3].

Chemical stimuli, light, and electric fields used to trigger redox processes are broadly applied external stimuli. Furthermore, electrochemical environments could in principle be used in combination with light excitation to control the conformation of the redox centre in successive or parallel steps. The use of a reference electrode in solution phase to control precisely the conformation of a supramolecular system by reduction or oxidation of a transition metal centre is thus quite different from the situation when a redox active molecule is inserted between a scanning tunnelling microscope (STM) tip and an electrode (two-electrode nanogap environments) and corresponds to the addition of a third 'gating' electrode [7]. Unfortunately, in addition to the merits of the resulting rigorous electrochemical control, achievable in solution phase, comes the need for using liquid environments. In a longer-term perspective this is not, however, necessarily a serious shortcoming. The electrochemical environment can be extended not only to a wealth of non-aqueous organic solvents but to both liquid and solid ionic media [8]. In a 'device' perspective, the latter may emerge as more suitable environments for electronically induced molecular-scale mechanical functions.

In this report we introduce a new working principle for externally triggered molecular-scale mechanical machines. Firstly, we combine the light-driven molecular machine function with an electrochemical environment. Secondly, in contrast to all previous reports on electrochemically driven conformational motion, electrochemical control occurs at the interface between two immiscible liquid electrolyte solutions, rather than on a solid electrode in contact with a single liquid electrolyte solution phase.

The interface of two immiscible electrolyte solutions (ITIES) is composed of two immiscible liquids (e.g. aqueous and organic phases) together with two electrolytes: one in each phase (ordinary inorganic ions, such as alkali halides, for the aqueous phase; hydrophobic organic ions, such as, for example, tetrabutylammonium hexafluorophosphate, for the organic phase) [9]. Importantly, under the influence of an electric field, two 'back-to-back' electrical double layers are formed on each side of the liquid/liquid interface. This interface can be polarized up to certain voltage drops, above which the traffic of ions across the interface starts [10]. Electric fields up to 0.5 V Å^{-1} localized at the interface can be achieved for typical ITIES.

Interest in ITIES was initially inspired by its role as (i) a medium for phase transfer catalysis [11], (ii) an environment for artificial photosynthesis and solar energy conversion [12], and (iii) as a model biomimetic system [12]. However, it was recently understood that functionalized ITIES can offer much more than that. Indeed, ITIES are ideal soft-matter environments for the self-assembly of nanoparticles, quantum dots, and supramolecular constructions [13]. These properties could be used for building nanometric molecular machines and electronic devices, operating at interfaces.
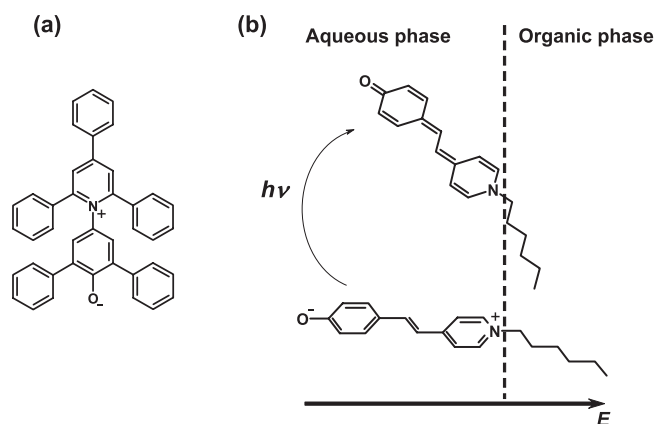
Figure 1. (a) The solvatochromic probe Reichardt's betaine; (b) a putative light-driven ITIES-based molecular machine based on a merocyanine dye anchored at the interface by a hydrophobic linking unit ('tail'). Light excitation results in a significant charge redistribution, causing the rotation of the chromophore from an upright to more recumbent position. The mechanical motion may be assisted or impeded by the external electric field.

Creation of molecular devices at ITIES offers a set of specific advantages.

(1) The localization of the molecule at the interface and the manipulation of the extent of molecular penetration into either of the phases can be tuned synthetically by changing the balance between the tailored hydrophobic and hydrophilic parts of the molecule.

(2) Both aqueous and organic phases are transparent to visible light, and this allows the use of optical excitation to induce a variety of processes in the probes localized at the interface.

(3) As a consequence of interface transparency to light, optical spectroscopic methods specific to interfacial phenomena can be employed to monitor the device function, e.g. second harmonic generation (SHG) spectroscopy [14, 15] or absorption and emission evanescence (total internal reflection mode) spectroscopy [16, 17].

(4) The electric field at ITIES is localized near the interface, in the back-to-back double-layer region. The field can be strong enough to affect the properties of the localized particles, their configuration at the interface, and their spectroscopic characteristics such as charge transfer absorption spectra.

(5) Since both sides of ITIES are liquid, it should be possible to build a truly self-assembled device which will transform the energy of light into mechanical motion. Since the system is self-assembled, its 'soft core' cannot be broken down; it will restore its properties after any perturbations.

(6) Thin-film or nano-fluidic devices can be designed on the basis of these principles.

In this report we shall describe the principles of operation of such a class of molecular machines. We discuss the criteria that are important for the design of suitable molecular architechtures. In order to be suitable for self-assembly at ITIES, molecules must have a combination of a hydrophobic functionality: a 'tail' residing in the oil phase and a polar 'head'-group residing in water. We consider head-groups in which intramolecular charge transfer can be induced by the absorption of visible light. This will lead to a substantial change in the dipole moment of the molecule (magnitude or direction or both). Examples of potential candidate architectures are given in figures 1 and 2 and discussed in more detail in section 2. An intramolecular electron transfer process, such as is shown in figure 2, is also included in this discussion, once it leads to a substantial charge rearrangement in the probe.
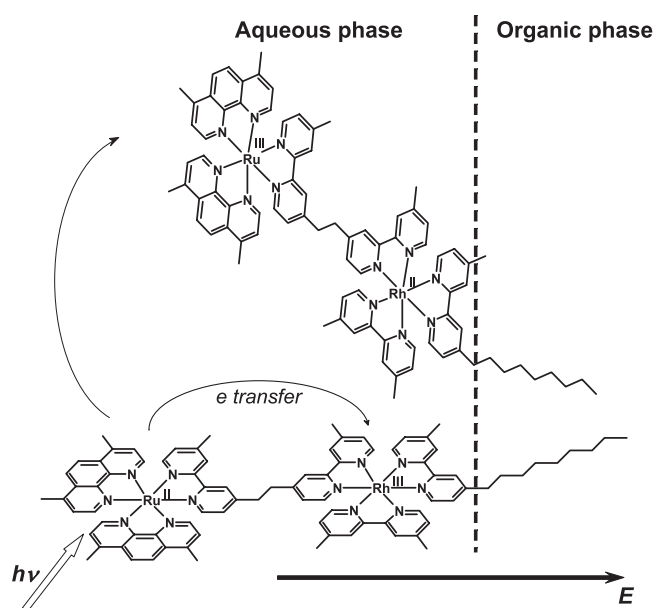
Figure 2. A mixed-metal Ru^{II}/Rh^{III} binuclear complex demonstrating the principle of the light-driven ITIES-based molecular machine. Light excitation is directed towards the Ru^{II} centre and is followed by electron transfer to the Rh^{III} moiety. This is accompanied by a conformational shift of this moiety towards an interface. Since the peripheral terminal is highly charged in both states, without an electric field the molecule should be oriented normal to the surface. A substantial negative field, as marked by the arrow, should be applied to ensure that the molecule rotates toward a flat orientation after the charge of the peripheral group increases from 2+ to 3+ following excitation.

The role of the electric field could be multifarious. According to the basic principles of light-induced intramolecular charge transfer, first formulated by Hush [18], the field may shift the absorption band maximum in either direction through its effect on the driving force of electron transfer. Furthermore, for a given direction of external field, the orientation of the head may no longer be favourable after the charge rearrangement. The head will then tend to bow, or erect, or thrust in the normal direction to the interface, depending on the character of charge transfer and the magnitude and direction of the field. If there is a bending degree of freedom between the head and the tail, the head will move alone; if not, it will tilt together with the tail, as far as the structural constraints allow, subject to the forces operating near the interface.

The important characteristic of the molecular machine is the reversibility of its function. In the present case, the charge rearrangement is induced by the absorption of a photon of light, and one of the following pathways will return the system to the initial charge state: fluorescence, thermal decay or back electron transfer. With the restoration of the initial charge state, the initial molecular orientation will also be restored. This suggests that timing of the events pertinent to device function is crucial, e.g. back electron transfer should not occur prior to the change in the orientation of the probe versus the interface.

In summary, tuning the external electric field will shift the light absorption frequency and change the mode of the motion of the molecule. Whereas it may be premature to discuss how this can be used practically as an 'opto-nano-mechanical' device, the electro-chromic capacity of such probes is obvious. Furthermore, if we extend this concept to monolayers of such molecules, the resulting system may offer features of a memory device. Last but not

least, such systems might constitute a promising model for the investigation of electron transfer, including electron transfer across the interface of ITIES.

2. Some molecular design principles of ITIES-based molecular teaspoon

The molecular machine that we describe performs bending motions in the plane perpendicular to the interface plane following light excitation, 'stirring' the interface of ITIES; thus we call it 'a molecular teaspoon'. Crucial molecular design elements of a molecular 'teaspoon' within our model are: (i) well-defined orientation at the interface, which is not significantly perturbed by thermal motion, at least when the interfacial electrical field is turned on; (ii) the electronically active moiety completely embedded on the aqueous side of the interface; (iii) the electronic charge distribution of the active element must undergo substantial re-distribution on light excitation, either associated with a large transition dipole or intramolecular electron transfer between two well-defined sites in a binuclear structure; and (iv) the electronic charge redistribution must not lead to significant translational motion across the interface, as this might lead to inhomogeneous broadening of spectral and other signals. Meeting these conditions requires some care in the molecular design and inevitably a demanding chemical synthesis strategy.

We note here that interfacial localization of the probe and fulfilment of the model requirements outlined above must be verified experimentally. Here we discuss two examples of molecules which might, in our view, constitute successful probes; figures 1 and 2. In both cases, interfacial anchoring is achieved through the combination of a strongly hydrophobic anchoring group such as a long aliphatic hydrocarbon chain with a hydrophilic charged moiety, which remains entirely in the aqueous phase in both the ground and excited electronic states.

The design of the polar photophysically active 'head' deserves special attention. An illustration is the organic chromophore betaine with a well-established dipole change following excitation; figure 1 [19]. Though polar in the ground state ($\mu = 15$ D), upon excitation the betaine moiety undergoes a tautomeric change leading to a change in the dipole moment, $\Delta\mu \approx -6$ D [20]. This property has been the basis for the solvatochromic hypersensitivity of betaines, used as a solvent polarity probe. The most widely used, 2,6-diphenyl-4-(2,4,6-triphenylpyridinium-1-yl)-phenolate, which is also known as Reichardt's betaine (figure 1(a)), cannot be used for ITIES-based molecular machines due to its low solubility in aqueous phase; however, the merocyanine analogue (e.g. figure 1(b)) and its derivatives, characterized by enhanced solubility in the aqueous phase [21], holds some promise.

Binuclear transition metal complexes [22, 23] of significant electrostatic charge may appear as an ultimately most promising strategic starting point. Such target molecules offer several merits, but also with some constraints:

(1) Versatile synthetic routes towards a wide range of photostable binuclear transition metal complexes.

(2) The photochemically active molecular part could be found in the interfacial region between aqueous and oil phases, especially in the presence of an external electric field, the magnitude of which can be used to control the degree of penetration from one phase to another [17]. In order to enhance the selectivity of the probe to the interfacial region, we envisage using the ligand sphere as a controlling factor, e.g. introducing long hydrophobic chains and/or hydrophilic groups such as $-COO^-$ to the periphery of the chromophores. The nature of a counterion for a transition metal centre might also be used to affect the phase preference.

(3) A variety of mixed metal binuclear transition metal complexes based on Os^{II}, Ru^{II}, Re^{I}, Rh^{III}, Pt^{II}, and Pd^{II} etc can be synthesized, and the difference in the electronic properties

of each redox centre can be used to achieve the desirable charge transfer characteristics, which are needed for ITIES-based molecular machines. We propose that the redistribution of charge is triggered by the localized excitation of one transition metal centre followed by fast intramolecular electron transfer. For this to take place, the binuclear complexes in question should be significantly structurally and electronically asymmetric. If this requirement is not fulfilled, excitation would result in the formation of mixed valence architectures. The tuning of the redox levels in transition metal centres is crucial, as demonstrated by the prevalence of energy transfer paths in Ru^{II}/Os^{II} binuclear complexes versus electron transfer in Ru^{II}/Os^{III} systems [23]. In our view, an energy transfer process would not offer a sufficient redistribution of charge to achieve a unidirectional change in orientation of the probe following excitation, therefore we propose to utilize the electron transfer, e.g. following excitation of a Ru^{II} centre in a binuclear Ru^{II}/Rh^{III} system, figure 2: $(Ru^{II})^*/Rh^{III} \rightarrow Ru^{III}/Rh^{II}$.

(4) The external electric field can be used to ensure and enforce a uniform orientation in the initial and final states of the probe.

(5) The nature of the bridging group between the two redox centres will play an important role. The electronic communication is key to enabling initial charge transfer, which would normally occur along the bridge [23], while sufficient separation of charges must be achieved to prevent fast back-electron transfer. In the longer term, bridge architectures should be considered, which could undergo structural reorganization following initial electron transfer. Presently, intermediate-length aromatic or aliphatic bridge groups appear to yield acceptable intermolecular electron transfer rates ($k = 1.7 \times 10^9$ for the probe shown in figure 2) [23].

The design principles summarized above pose significant synthetic challenges that are, however, likely to come within reach. We will now discuss the theoretical basis of the operation of such kinds of devices assembled at interfaces.

3. Model and general equilibrium characteristics

A simplified model of the head-group localized in the aqueous phase is shown in figure 3. It consists of two distinct regions with accumulated positive and negative charge, depicted by groups 1 and 2 in the present consideration. The exact position of the head relative to the interface is determined by the balance of hydrophilic and hydrophobic forces and the electric field direction (if present). For simplicity, we shall assume that the head is anchored at and can bend about the point where the molecule penetrates the dividing surface (figure 3). Bending or rotation of the head about this point are, of course, limited by the finite size of the head.

In the absence of an external field, the average orientation of the molecule is determined by all the interactions of the molecule with its environment at the interface. For simplicity, we will consider the molecules with an axially symmetric hydrophilic head (extension is straightforward). The orientation of the head without an electric field for such molecules will be perpendicular to the interface. Indeed, such an orientation corresponds to the minimum in the free energy of the system in view of a better solution of the charged groups with an increase in their distance from the interface. When an electric field of appropriate direction is applied perpendicular to the interface, this may result in a change in the equilibrium orientation of the molecule. Such electric fields appear as a result of the potential drop across the interface. Typical ITIES can sustain about 0.5 V of applied voltage. The orientation of the molecule can be found from the minimum of the free-energy functional, which, in view of azimuthal symmetry at the liquid–liquid interface, depends only on the angle α between the molecular
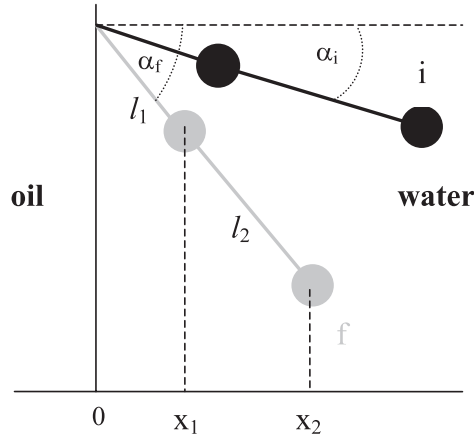
Figure 3. A sketch of the liquid/liquid interface with a molecule possessing an elongated hydrophilic head, residing in the aqueous phase, with two distinct regions—1 (close to the interface) and 2 (deep in the aqueous phase)—and a hydrophobic tail in the oil phase. α is the angle between the main axis of the head (which may coincide with the molecular axis, if the molecule is rigid) and the normal to the surface. The groups may be charged.

axis and the normal to the interface. This has the form

$$H = ez_1\Phi(x_1) + ez_2\Phi(x_2) + W_1(x_1) + W_2(x_2) + K\alpha^2 \tag{1}$$

where $x_1 = l_1\cos\alpha$ and $x_2 = l_2\cos\alpha$ (see figure 3). Here $\Phi(x)$ is the electrostatic potential distribution in the water phase; the W-terms are the self-energies of the charged groups, which are determined mainly by the image force energies near the interface; the last term is an elastic energy due to hydration repulsion beyond the image forces and, possibly, intramolecular rigidity (for simplicity, we do not consider anharmonic terms). The value of the 'elastic constant' K depends on the nature of the molecule and both solvents. For estimation, we shall assume a value of about $0.5\,k_\mathrm{B}T\,\mathrm{rad}^{-2}$ for K.

All electrostatic interactions are screened by the ions of the supporting electrolyte. Much effort has been devoted recently to understanding the potential distribution at ITIES. For our purposes, it will be sufficient to use the simplest variant of the nonlinear Gouy–Chapman theory [24]. Accordingly, the potential distribution in the aqueous half-space will be taken in the form,

$$\Psi(x) = 2\ln\left\{ \frac{1 + \frac{e^{\Psi_0/2}-1}{e^{\Psi_0/2}+1}e^{-\kappa_\mathrm{w}x}}{1 - \frac{e^{\Psi_0/2}-1}{e^{\Psi_0/2}+1}e^{-\kappa_\mathrm{w}x}} \right\}. \tag{2}$$

Here we introduce dimensionless potentials

$$\Psi(x) \equiv \frac{e\Phi(x)}{k_\mathrm{B}T}, \qquad \Psi_0 \equiv \frac{e\Phi_0}{k_\mathrm{B}T} \tag{3}$$

with $\Phi_0 \equiv \Phi(x=0)$ being the potential drop between the surface and the bulk of the aqueous phase; κ_w^{-1} is the Debye length in the aqueous phase.

Hereafter, in order to demonstrate the possible effects, we will operate with Ψ_0 as a controlled value. However, in experiments, the overall potential drop between the bulk of the organic and aqueous phases is controlled:

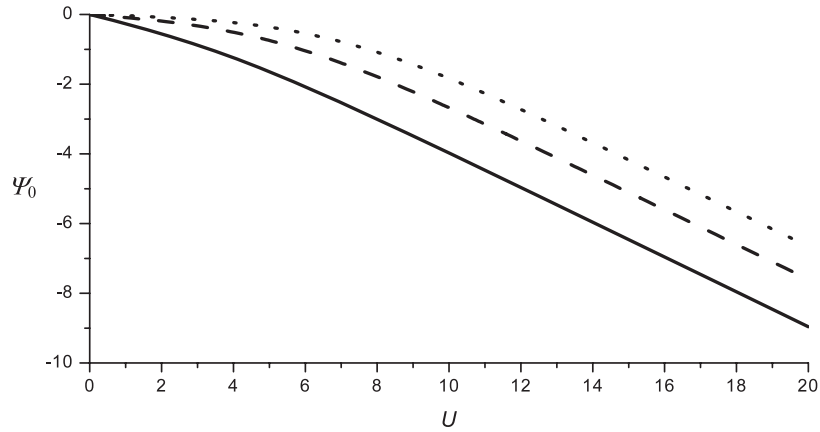$$U \equiv \frac{e\left[\Phi(-\infty) - \Phi(\infty)\right]}{k_\mathrm{B}T}. \tag{4}$$

Figure 4. Dependence of potential drop in the aqueous phase, Ψ_0, on the overall potential drop U calculated for the 1,2-dichlorethane–water interface at three different concentrations of the electrolyte in the organic phase: 0.1 (solid line), 0.01 (dotted line) and 0.001 M (dashed line). Concentration of the electrolyte in the aqueous phase, is 0.1 M. $\varepsilon_w = 80$, $\varepsilon_o = 10$. All potentials are given in units of $k_B T/e$, which is 25 mV at room temperature.

The value of Ψ_0 may be calculated through the value of U, using the model of two back-to-back double layers, namely the Verwey–Niessen model [25, 26]:

$$\Psi_0 = 4 \tanh^{-1} \left\{ \frac{\sqrt{1 + \gamma e^{U/2}} - \sqrt{1 + \gamma e^{-U/2}}}{\sqrt{1 + \gamma e^{U/2}} + \sqrt{1 + \gamma e^{-U/2}}} \right\} - U \tag{5}$$

where

$$\gamma \equiv \frac{\varepsilon_w \kappa_w}{\varepsilon_o \kappa_o} \tag{6}$$

with κ_o^{-1} being the Debye length in the organic phase, and ε_w and ε_o being the water and oil dielectric constants (Gaussian units are used). Figure 4 shows the dependence of Ψ_0 on the overall potential drop U for the 1,2-dichlorethane/water interface at three different concentrations of the electrolyte in the organic phase. One can see that, for $U = 0.6$ V and concentrations of 0.01 M and higher in the organic phase, the absolute value of the potential Ψ_0 may reach 250 mV.

The image force energy W under the assumption of validity of macroscopic electrostatics may be roughly estimated by the following equation:

$$W(x) = \frac{e^2 z^2}{4 \varepsilon_w x} \mu \exp(-\kappa_w x), \qquad \mu = \frac{\varepsilon_w - \varepsilon_o}{\varepsilon_w + \varepsilon_o}. \tag{7}$$

Since $\varepsilon_w > \varepsilon_o$, equation (7) describes the repulsion of the charge (of any sign) located in water from the interface, screened by electrolyte. Equation (7) oversimplifies the screening of the charge imbedded in a highly inhomogeneous distribution of ions near the interface. This equation may be considered as an extrapolation formula since, when the ion is located very close to the interface, it is still weakly screened, whereas the screening approaches the bulk-like Debye law when the charge is located at a long distance from the interface.

The equilibrium orientation of the molecule at a given charge distribution is determined by the condition
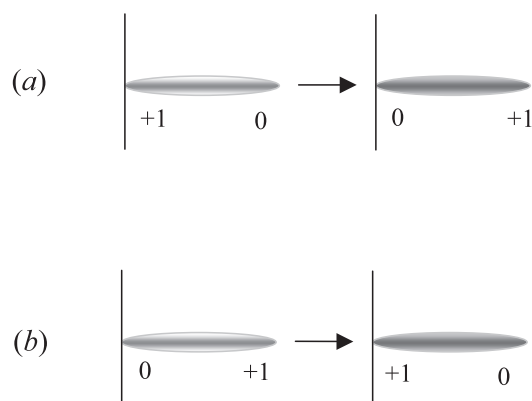
$$\partial H / \partial \alpha = 0. \tag{8}$$

Figure 5. A scheme for the intramolecular flip-flop of the charge under light illumination: (a) outward charge transfer; (b) inward charge transfer.

After substitution of equation (1) into (8), one may find numerically the equilibrium angle, α_{eq}, at different potentials Ψ_0. Generally, the solutions of equation (8) may correspond to stable, metastable and unstable configurations. A stability analysis for each particular system must therefore be performed. We shall show this for the particular case considered in the next section.

It should be emphasized that the equilibrium value of the angle depends on the charge distribution within the molecule. If the charge is relocated within the molecule as a result of light-induced intramolecular electron transfer or reaction with redox species, the equilibrium orientation may therefore be different in the initial and final states.

4. Example: intramolecular 'flip-flop' of the charge

The solutions of equation (8) are relatively simple when the charge of one of the two groups is equal to zero in the initial (ground state before illumination) or final (excited) state. We therefore now consider two particular cases of the intramolecular electron transfer of the type shown in figure 5.

(1) *Outwards charge transfer.* Here (figure 5(a)) we have

$$z_1^i = z_2^f = 1; \quad z_1^f = z_2^i = 0 \tag{9}$$

where the superscripts i and f denote the initial and final states. For this case, one may find the analytical solution of equation (8) for Ψ_0 as a function of α_{eq}, and then plot α_{eq} versus Ψ_0. Figure 6 shows the $\alpha_{eq}(V)$ dependence, where $V = -\Psi_0$, so that for a negatively polarized interface, $V > 0$.

As figure 7 shows, there is always a solution $\alpha = 0$, but it is not always the equilibrium one. For the initial state above a critical value, V_{cr}, this solution becomes unstable, and the stable solution is described by the growing curve branch of curve i. For the final state (figure 6, curve f) there are two critical values, $V_{cr}^{(1)}$ and $V_{cr}^{(2)}(> V_{cr}^{(1)})$, different from the above one (both substantially lower). At $V > V_{cr}^{(1)}$, a solution with $\alpha \neq 0$ corresponds to a second minimum of the H(d) curve, separated from the $\alpha = 0$—minimum by a barrier, the position of the maximum of which is determined by the third solution. Somewhere in the range $V_{cr}^{(1)} < V < V_{cr}^{(2)}$ the first minimum, the one at $\alpha = 0$, becomes metastable, and then totally unstable. However, of crucial importance for the present study is the following. Within the realistic interval of potential drops
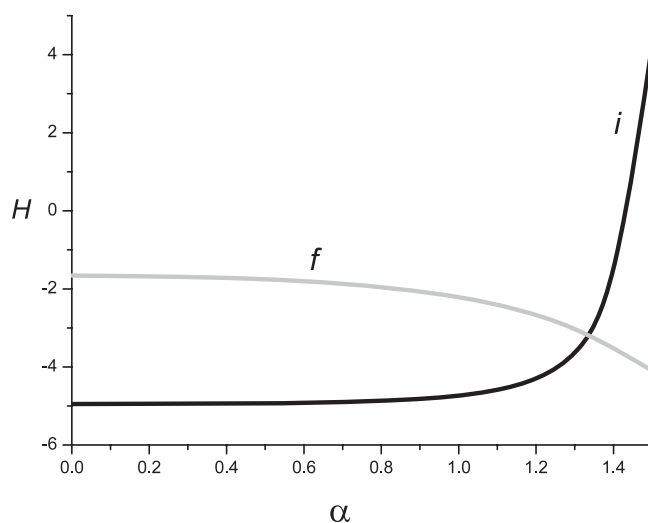
9

Figure 6. Dependence of the free energy of the system on the orientation of the molecule for the outward charge transfer according to the scheme in figure 5(a) in the initial (i) and final (f) states. $V = 10, \kappa l_B = 0.7$ (l_B is the Bjerrum length), $\mu = 0.5\,k_B T/\mathrm{rad}^2$, $K = 0.5$. For the inwards charge transfer the situation is the reverse.
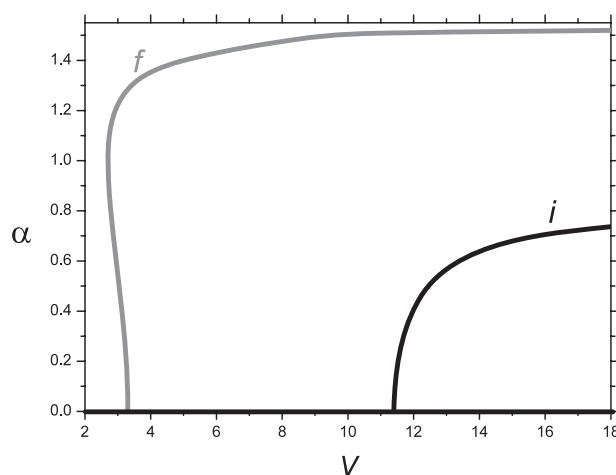

Figure 7. Equilibrium angle as a function of $V = -e\Phi_0/k_B T$, the dimensionless potential drop in the aqueous phase (with a minus sign) for the initial (i) and final (f) states for outwards charge transfer. The values of the parameters are the same as in figure 6. At $V < 11.4$ for the initial state and $V < 2.6$ for the final state, the equilibrium angle is zero. In the interval $2.6 < V < 3.25$ there are three solutions for the orientation in the final state. Two of them correspond to the minima on the free-energy curve, and the third one determines the position of the barrier maximum between them. For the inwards charge transfer, the curves for the initial and final states are swapped.

(approximately 90 mV $< V <$ 300 mV), the stable solution in the initial state (ground state) and the stable solution in the final state (achieved following excitation) are different; figure 7. Thus, following excitation, α will change: the head will tilt from $\alpha_{eq} = 0$ to some larger value. For large enough V, this value tends to $\alpha_{eq} = \pi/2$. The zero angle in the initial state remains unchanged for all practically achievable potentials, whereas the saturation to $\pi/2$ in the final

state is achieved at approximately 100 mV: a further increase in the field will practically not affect the result. This feature is a consequence of the special character of the nonlinear Gouy–Chapman screening. The dominant part of the counterions is drawn very close to the surface, while the rest of the field is a tail of the Debye-like decaying field. So the effect on the group 2, imbedded deep into the aqueous phase, is relatively weak, and it varies weakly with the potential.

(2) *Inwards charge transfer* (figure 5(b)). Here the superscripts i and f in equation (9) should be interchanged. The ground state corresponds to the localization of the charge on group 2, whereas the charge transfer excited state corresponds to the charge on group 1. The situation is thus opposite to the first case, and in the initial state the orientation of the molecule is almost parallel to the surface for large enough potentials. Light absorption results in a change in the orientation to that perpendicular to the surface.

This case is of additional interest from a different perspective. The molecule can change its orientation due to the change in the value of the potential drop without illumination. Indeed, as seen from figure 7, the off switching of the electric field results in a drop of the equilibrium angle to zero. It is important that both states are stable, and this may facilitate their experimental discrimination.

If the initial state corresponds to parallel orientation, we cannot expect any noticeable electrochromic effect. However, after illumination the relaxation will cause a time-dependent shift in a spectroscopic signal such as fluorescence, *vide infra*, in a similar way to that in the first case.

5. Light absorption

The position of the maximum of the light absorption corresponding to intramolecular charge transfer is given by

$$\hbar\omega_{max}^{ab} = e[z_1^{(f)} - z_1^{(i)}]\Phi(x_1^{(i)}) + e[z_2^{(f)} - z_2^{(i)}]\Phi(x_2^{(i)})$$
$$+ W^{(f)}(x_1^{(i)}) - W^{(i)}(x_1^{(i)}) + W^{(f)}(x_2^{(i)}) - W^{(i)}(x_2^{(i)}) + E_0 \tag{10}$$

where E_0 is the intrinsic transition energy for the molecule in the aqueous phase in the absence of an electric field. Let us consider the potential-dependent part of the absorption band maximum:

$$\Delta(V) = \hbar\omega_{max}^{ab}(V) - \hbar\omega_{max}^{ab}(0). \tag{11}$$

For the *outwards charge transfer* (the first example in section 4),

$$\Delta(V) = e\Phi(x_2^{(i)}) - e\Phi(x_1^{(i)}) \tag{12}$$

where we neglected the possible weak dependence of the equilibrium angle (and hence $x_1^{(i)}$ and $x_2^{(i)}$) on the potential drop.

This, however, may be of importance for the *inward charge transfer*, where all terms in equation (10) should be taken into account. Then,

$$\Delta(V) = e\Phi(x_1^{(i)}) - e\Phi(x_2^{(i)}) + W^{(f)}(x_1^{(i)}) - W^{(f)}(l_1) + W^{(i)}(l_2) - W^{(i)}(x_2^{(i)}). \tag{13}$$

Figure 8 shows the typical dependence of $\Delta(V)$ for outwards (a) and inwards (b) charge transfer. Moderate shifts are demonstrated (up to the maximum of about 1000 cm^{-1} at 0.5 V) but such shifts are detectable in optical experiment [15]. Whereas the character of the electrochromic effect in (a) is obvious, the peculiar behaviour in (b) has the following reason. At small fields the molecule stands perpendicular to the interface, and Δ decreases with negative polarization of the interface (curve 1). Once the orientation of the molecule
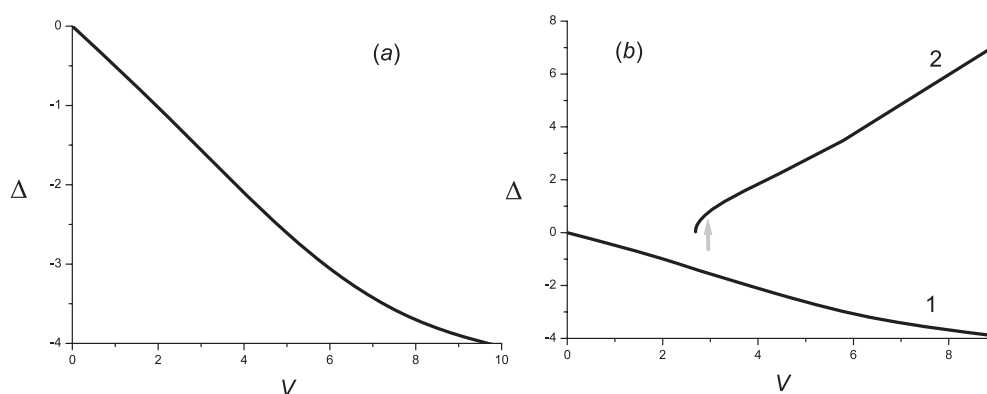
Figure 8. Dependence of the electrochromic shift of the light absorption maximum on the potential drop (equation (11)), given in units of $k_B T$, plotted for outwards (a) and inwards (b) charge transfer. Same parameter values as in figure 6. For the inward transfer the expected complicated behaviour is due to a transition between two orientational states (see text).

jumps to a tilted state, a further increase in the negative potential will draw the second group closer to the interface, and this will cause the increase in Δ (curve 2). The transition between the two states will be affected by fluctuations and will take place somewhere in the vicinity of the arrow shown.

One of the methods for the study of potential-dependent light absorption by interface-localized molecules is the electromodulation technique. This protocol allows separation of the contribution of the interfacial region from the bulk contribution through the derivatives with respect to the potential drop. The latter should affect only the interfacial properties. For s-polarized light, the corresponding derivative of the reflection coefficient associated with the adsorbed molecules reads [27]

$$\frac{1}{R_s}\frac{\mathrm{d}R_s}{\mathrm{d}U} = -16\pi N\frac{\omega}{c}\cos\theta\frac{\sqrt{\varepsilon_w(\omega)}}{\varepsilon_w(\omega) - \varepsilon_o(\omega)}\frac{\mathrm{d}p}{\mathrm{d}U} \tag{14}$$

where N is the number of adsorbed molecules per unit area, ω and c are the frequency and velocity of light, $\varepsilon_w(\omega)$ and $\varepsilon_o(\omega)$ are the optical dielectric constants of the aqueous and organic solutions (practically, of water and oil), and θ is the angle of incidence. The imaginary part of optical polarizability of the adsorbed molecule, p, depends on the potential drop across the interface due to the electrochromic effect discussed above. In the Lorentz approximation, we have

$$\frac{\mathrm{d}p}{\mathrm{d}U} \propto \frac{(\omega - \omega_{max}^{ab}(U))}{[(\omega - \omega_{max}^{ab}(U))^2 + \Gamma^2]^2}\frac{\mathrm{d}\omega_{max}^{ab}(U)}{\mathrm{d}U} \tag{15}$$

where Γ is the width of the absorption band. Equations (14) and (15) show that the electroreflectance signal vanishes at a frequency corresponding to the absorption band maximum. This allows determination of the dependence of ω_{max}^{ab} on the potential drop and comparison with theory (equations (12), (2), and (5)).

Note that equations (14) and (15) refer to a signal from the adsorbed molecules. This must be distinguished from the contribution that may come from the interface itself, which is expected to be small in the achievable potential range and, if any, the signal should appear at a different frequency.

Second harmonic generation (SHG) spectroscopy is a well-established nonlinear optical technique for probing ordered phases, such as liquid/liquid interfaces, which allows us to

selectively detect the signal coming from the interfacial region without a contribution from the bulk solution [14]. The SHG signal is generated at the interface and detected at twice the fundamental frequency of the excitation source ($2h\nu$). The SHG intensity is greatly enhanced when the harmonic frequency ($2h\nu$) is tuned to the frequency of the electronic transition. The absorption spectra of species localized at the interface could be measured. In the present context it could be used to detect the change in absorption frequency of charge transfer transition resulting from the application of electric field across the interface; cf equations (11)–(13).

Attenuated total internal reflection (ATR) absorption spectroscopy could be used to monitor the same effect [16, 17], with the difference that the position of the absorption band is detected by measuring the intensity of the same frequency as that used for irradiation ($h\nu$). Both SHG and ATR absorption and fluorescence measurements can be performed in time-resolved mode, allowing us to monitor the changes in spectroscopic properties arising from excitation and subsequent mechanical motion. In the next section, we consider the changes which might be observed in time-resolved fluorescence measurements as an example.

6. Time-dependent fluorescence

Since, immediately after light absorption at sufficiently strong external electric fields, the molecule may assume a non-equilibrium orientation, the tilt angle will start to relax to the new equilibrium position. If we assume that excitation leads to an emitting excited state and fluorescence is the main pathway for the dissipation of the excited state energy, the emission maximum will therefore depend on time t due to the change in tilt angle according to equation [28]

$$\hbar\omega_{max}^{em}(t) = E_0 + H^{(f)}(s(t)) - H^{(i)}(s(t)) \tag{16}$$

where $s(t) = \cos\alpha(t)$.

If the radiation life-time of the excited state is sufficiently long, the fluorescence could also be observed from the final equilibrium configuration to which the system will relax. The maximum of the fluorescence from this configuration will be equal to

$$\hbar\omega_{max}^{em}(\infty) = E_0 + H^{(f)}(s^{(f)}) - H^{(i)}(s^{(f)}) \tag{17}$$

where $s^{(f)}$ is the final equilibrium value, and $H^{(f)}(s)$ and $H^{(i)}(s)$ are the free energies of the final and initial states at arbitrary angles.

Note that the shift in the fluorescence maximum prescribed by these equations will occur on a slower timescale than the femtosecond solution dynamics, because it originates from substantially slower rotation of a large 'head'-group or a molecule as a whole. Since the $H^{(f)}(s^{(f)})$ and $H^{(i)}(s^{(f)})$ may depend on the potential drop, an *electrochromic effect* on the fluorescence may also be observed.

Generally, time dependence of $s(t)$ may be rather complicated, as it depends not only on the forces considered here, but also on the interaction with molecular surroundings, such as the solvent. As a crude approximation, a simple exponential form may be used

$$s(t) = s_f + (s_i - s_f)\exp(-t/\tau) \tag{18}$$

where τ is the relaxation time. This dependence is shown in figure 9 for the particular case shown in figure 5(a). The electrochromic effect in the final state is of the same order as the electrochromic effect in the light absorption (figure 8).

7. Concluding remarks

In this report we have introduced a working principle for a new type of molecular machine that can convert the energy of light and/or an electric field into mechanical motion. The operation
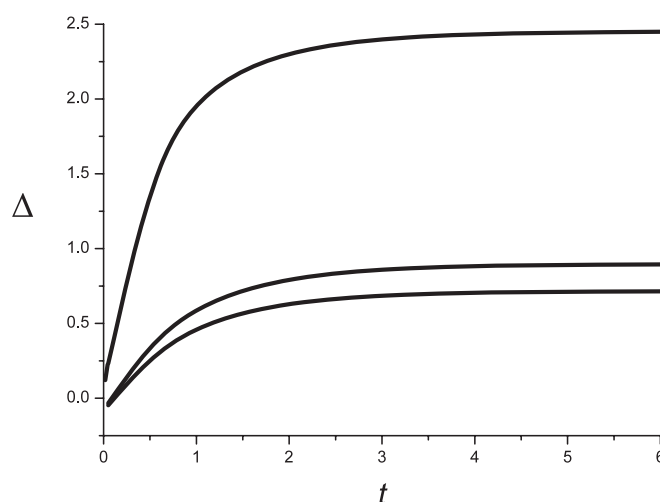
Figure 9. Time dependence of the fluorescence maximum for various values of the potential drop (according to equations (16), (18)), both given in units of $k_{\mathrm{B}}T$; time is given in the units of relaxation time τ. The results are shown for the outwards charge transfer. The case of inwards charge transfer reverses the dependence. Curves: $V = 3(1),\ 5(2),\ 10(3)$. Other parameters are the same as in figure 6.

relies on immobilization of the molecular entity at an ITIES and the motion can be controlled by the electric field across the interface. For such a machine a molecule with a hydrophilic head that exhibits light-induced intramolecular electron transfer, attached to a hydrophobic tail, is needed. The hydrophilicity and hydrophobicity of the molecule should be balanced to maintain localization of the molecule at the interface. In contrast to previous opto-mechanical molecular machines, the device operation is thus entirely in a liquid state environment and a high order of self organization, stable to external perturbation, is achieved. Our analysis for such systems suggests that:

- The orientation of the molecule can change after illumination by an angle of up to 90° for quite realistic structures. The molecule will return to its initial state following excited state deactivation (via fluorescence emission or non-radiative decay) or back-electron transfer. The motion could be followed by time-resolved spectroscopic methods, e.g. fluorescence spectroscopy.
- The system exhibits electrochromic properties that can be studied by second harmonic generation spectroscopy, attenuated total internal reflection spectroscopies or optical electromodulation spectroscopy (electroreflectance has been considered presently). The range of potential drops able to control these phenomena lies in an achievable potential window, from 200 to 500 mV, which are available for ITIES.
- Furthermore, the orientation of the molecule at ITIES can be obtained by determining the three components of the susceptibility tensor from analysis of the SHG intensity as a function of the fundamental beam ($h\nu$) polarization angle for the s- and p-polarised SHG outputs [14, 29]. Since such analysis requires taking into account the molecular symmetry of the interfacially localized probe, it was not considered here in detail.

The working principle is novel for a molecular mechanical device ('machine') and we have provided in some detail appropriate theoretical background. Routes towards implementation of

these concepts into a working device involve, however, issues that are only partly clarified, particularly:

- Design of molecular systems. Some design principles and molecular system classes that accord with the new working principle were noted in section 2. Binuclear transition metal complexes, transition metal complexes in supramolecular conjunction with organic redox moieties (e.g. including fullerenes), and suitably derivatized organic charge transfer molecules were noted as attractive candidates. Although laborious, their chemical synthesis is within the reach of known approaches and strategies. In the context of real molecular systems that accord with the ITIES-based conceptual and theoretical principles suggested, molecular design therefore appears as a tractable issue.

- A second, presently more elusive issue is related to the multiple energy conversion steps needed for cyclic molecular machine function. As in most real or putative molecular machine constructs, rational energy conversion involves at least two steps. The first generic step is the conversion of externally (abundantly available) energy such as light energy to the localized molecular-based mechanical motion. The estimated energy required for this step exceeds that available from thermal motion ($k_B T$). The novel molecular system design here offers clear conversion principles for this step. As in other molecular machines, the second step, namely transduction of the locally induced mechanical molecular response to rational work, is less transparent. So far, the principles for this step in the overall conversion of externally supplied energy to useful work have been clarified only when solid-state interfaces are involved. Light-induced *cis–trans* transition of azobenzene incorporated in a peptide chain linked to the tip in an AFM configuration is such an example. Light energy is first converted to a configurational change in the chain. In a second step the configurational change is transduced to mechanical energy stored in the AFM cantilever [30]. In a related system the primary energy conversion step is achieved by interfacial electrochemical electron transfer to a ferrocene-based linear polymer. Oxidation of the ferrocene units induces conformational structural changes in the polymer, again transducing to energy storage in an AFM cantilever [31].

- Similarly, the immediate most obvious speculations about the second-step for the present machine could be based on an extension of the ITIES concept, in which the electronically active molecules are confined at the interface between the bulk aqueous solution and a thin film of organic solvent in contact with a solid surface. The latter could again be an AFM cantilever with a concomitant second-step mechanical response. It could, however, also be an electrochemical metallic interface. The light- or field-induced configurational changes at the ITIES could be monitored in either case, by mechanical cantilever deflection or by optical and electrochemical signals at the solid/liquid film interface, respectively. The model and concepts introduced can be extended further, but this is hardly warranted before the basic idea has been verified experimentally.

Acknowledgments

References

[1] Telford J R, Wittung-Stafshede P, Gray H B and Winkler J R 1999 *Acc. Chem. Res.* **31** 755
[2] For a review, see Wolf E L 2004 *Nanophysics and Nanotechnology An Introduction to Modern Concepts in Nanoscience* (Weinheim: Wiley–VCH)
[3] For a overview, see Balzani V, Venturi M and Credi A 2003 *Molecular Devices and Machines A Journey into the Nanoworld* (Weinheim: Wiley–VCH)
[4] Saha F and Stoddart J F 2007 *Chem. Soc. Rev.* **36** 77
[5] Beckmann R, Beverly K, Boukai A, Bunimovich Yu, Choi J W, DeIonno E, Green J, Johnston-Halperin E, Luo Y, Sheriff B, Stoddart J F and Heath J R 2006 *Faraday Discuss.* **131** 9
[6] Collier C P, Jeppesen J O, Luo Y, Perkins J, Wong E W, Heath J R and Stoddart J F 2001 *J. Am. Chem. Soc.* **123** 12632
[7] Albrecht T, Guckian A, Ulstrup J and Vos J G 2005 *Nano Lett.* **5** 1451
[8] Albrecht T, Moth-Poulsen K, Christensen J B, Hjelm J, Bjørnholm T and Ulstrup J 2006 *J. Am. Chem. Soc.* **128** 6574
[9] Samec Z and Kakiuchi T 1995 *Adv. Electrochem. Electrochem. Sci.* ed H Gerischer and C W Tobias (Weinheim: VCH) p 297
[10] Girault H H and Schiffrin D H 1989 *Electroanalytical Chem.* vol 15, ed A J Bard (New York: Dekker) p 1
    Girault H H 1993 *Modern Aspects of Electrochem.* vol 25, ed J O'M Bockris *et al* (New York: Plenum) p 1
[11] Starks C M, Liotia C L and Halpern M 1994 *Phase Transfer Catalysis* (New York: Chapman and Hall)
[12] Volkov A G, Deamer D W, Tanelian D I and Markin V S 1998 *Liquid Interfaces in Chemistry and Biology* (New York: Wiley)
[13] Su B, Abid J-P, Fermin D J, Girault H H, Hoffmannova H, Krtil P and Samec Z 2004 *J. Am. Chem. Soc.* **126** 915
[14] Corn R M and Higgins D A 1994 *Chem. Rev.* **94** 107
    Eisenthal K B 1996 *Chem. Rev.* **96** 1343
[15] Steel W H and Walker R 2003 *Nature* **424** 296
[16] Perera J M, Stevens G W and Grieser F 1995 *Colloids Surf.* A **95** 185
    Ishizaka S, Kim H-B and Kitamura N 2001 *Anal. Chem.* **73** 2421
[17] Ding Z, Wellington R G, Brevet P F and Girault H H 1996 *J. Phys. Chem.* **100** 10658
[18] Hush N S 1968 *Electrochim. Acta* **13** 1005
    Hush N S 1967 *Prog. Inorg. Chem.* **8** 391
[19] Kjær A M and Ulstrup J 1987 *J. Am. Chem. Soc.* **109** 1934
    Reichardt C 1988 *Solvents and Solvent Effects in Organic Chemistry* (Weinheim: VCH)
[20] Masternak A, Wenska G, Milecki J, Skalski B and Franzen S 2005 *J. Phys. Chem.* A **109** 759
[21] Martins C T, Lima M S and El Seoud O A 2005 *J. Phys. Org. Chem.* **18** 1072
[22] De Cola L and Belser P 1998 *Coord. Chem. Rev.* **177** 301
[23] Barigelletti F and Flamigni L 2000 *Chem. Soc. Rev.* **29** 1
[24] Schmickler W 1996 *Interfacial Electrochemistry* (New York: Oxford University Press)
[25] Verwey E J W and Niessen K F 1939 *Phil. Mag.* **28** 435
[26] Volkov A G and Markin V S 2002 *Encyclopaedia of Electrochemistry* vol 1, ed E Gileadi and M Urbakh (Weinheim: Wiley–VCH) p 162
[27] Brodsky A M, Daikhin L I and Urbakh M I 1984 *J. Electroanal. Chem.* **171** 1
[28] Maroncelli M, McInnis J and Fleming G R 1989 *Science* **243** 1674
    Simon J D 1988 *Acc. Chem. Res.* **21** 128
[29] Naujok R R, Higgins D A, Hanken D G and Corn R M 1995 *J. Chem. Soc. Faraday Trans.* **91** 1411
    Perrenoud-Rinuy J, Brevet P F and Girault H H 2002 *Phys. Chem. Chem. Phys.* **4** 4774
[30] Neuert G, Hugel T, Netz R R and Gaub H E 2006 *Macromolecules* **39** 789
[31] Butt H-J 2006 *Macromol. Chem. Phys.* **207** 573